

KAPL--4716

DE91 004969

## DISCLAIMER

This report was prepared as an account of work sponsored by an agency of the United States Government. Neither the United States Government nor any agency thereof, nor any of their employees, makes any warranty, express or implied, or assumes any legal liability or responsibility for the accuracy, completeness, or usefulness of any information, apparatus, product, or process disclosed, or represents that its use would not infringe privately owned rights. Reference herein to any specific commercial product, process, or service by trade name, trademark, manufacturer, or otherwise does not necessarily constitute or imply its endorsement, recommendation, or favoring by the United States Government or any agency thereof. The views and opinions of authors expressed herein do not necessarily state or reflect those of the United States Government or any agency thereof.

## Zinc(II) Oxide Solubility and Phase Behavior in Aqueous Sodium Phosphate Solutions at Elevated Temperatures

S. E. Ziemniak

M. E. Jones

K. E. S. Combs

February 1990

Prepared for  
The United States Department of Energy  
Assistant Secretary for Nuclear Energy  
Deputy Assistant Secretary for Naval Reactors

Prepared by  
General Electric Company  
KNOLLS ATOMIC POWER LABORATORY  
Schenectady, New York

Contract DE-AC12-76SN00052

**MASTER**  
DISTRIBUTION OF THIS DOCUMENT IS UNLIMITED

## DISCLAIMER

This report was prepared as an account of work sponsored by an agency of the United States Government. Neither the United States Government nor any agency thereof, nor any of their employees, makes an warranty, express or implied, or assumes any legal liability or responsibility for the accuracy, completeness, or usefulness of any information, apparatus, product, or process disclosed, or represents that its use would not infringe privately owned rights. Reference herein to any specific commercial product, process, or service by trade name, trademark, manufacturer, or otherwise, does not necessarily constitute or imply its endorsement, recommendation, or favoring by the United States Government or any agency thereof. The views and opinions of authors expressed herein do not necessarily state or reflect those of the United States Government or any agency thereof.

## CONTENTS

	<u>Page No.</u>
ABSTRACT.....	v
INTRODUCTION.....	1
EXPERIMENTAL.....	2
Materials.....	2
Apparatus.....	4
Procedures.....	4
RESULTS.....	8
Solubility Data.....	8
Thermodynamic Analysis.....	8
DISCUSSION.....	15
Zinc Oxide Dissolution into $Zn(OH)_2(aq)$ .....	15
Zn(II) Ion Hydrolysis.....	22
ZnO/NaZnPO <sub>4</sub> Transformation.....	26
Zn(II) Ion Phosphatocomplex Formation.....	29
REFERENCES.....	34

## ILLUSTRATIONS

### Figure No.

- 1 Schematic of flowing autoclave system used in zinc oxide solubility investigation
- 2 Comparison of measured and fitted solubilities of zinc oxide in sodium phosphate solutions (Na/P = 2.3)
- 3 Comparison of measured and fitted solubilities of  $\text{NaZnPO}_4$  in sodium phosphate solutions (Na/P = 2.3)
- 4 Comparison of measured and fitted solubilities  $\text{NaZnPO}_4$  in sodium phosphate solutions (phosphate = 10.5 mmol/kg)
- 5 Free energy changes measured during zinc oxide dissolution
- 6 Comparison of free energy changes associated with  $\text{Zn(II)}$  ion hydrolysis reactions
- 7 Comparison of measured and fitted solubilities of zinc oxide in sodium hydroxide solutions.
- 8 Standard entropies for  $\text{Zn(II)}$  and  $\text{Cu(II)}$  ions and their hydroxocomplexes
- 9 Predicted phase boundary for  $\text{ZnO}/\text{NaZnPO}_4$  transformation in aqueous sodium phosphate solutions
- 10 Distribution of  $\text{Zn(II)}$  ion complexes present in solution at 298 K (top) and 560 K (bottom) (Na/P = 2.3)

## TABLES

### Table No.

- I. Feedwater Compositions
- II.  $\text{ZnO}$  Bed Transformation Effects
- III. Measured  $\text{ZnO}/\text{NaZnPO}_4$  Solubilities in Aqueous Sodium Phosphate Solutions
- IV. Dissociation Behavior of Selected Compounds
- V. Thermodynamic Equilibria for Calculation of  $\text{ZnO}/\text{NaZnPO}_4$  Solubilities in Alkaline Sodium Phosphate Solutions via  $\Delta G(T) = A - BT - CT \ln T$
- VI. Thermochemical Parameters for Species in the  $\text{ZnO}-\text{H}_2\text{O}$  System
- VII. Thermochemical Parameters for Phosphate-Based Species in the  $\text{ZnO}-\text{Na}_2\text{O}-\text{P}_2\text{O}_5-\text{H}_2\text{O}$  System

## ABSTRACT

A platinum-lined, flowing autoclave facility is used to investigate the solubility/phase behavior of zinc(II) oxide in aqueous sodium phosphate solutions at temperatures between 290 and 560 K. ZnO solubilities are observed to increase continuously with temperature and phosphate concentration. At higher phosphate concentrations, a solid phase transformation to NaZnPO<sub>4</sub> is observed. NaZnPO<sub>4</sub> solubilities are retrograde with temperature.

The measured solubility behavior is examined via a Zn(II) ion hydrolysis/ complexing model and thermodynamic functions for the hydrolysis/complexing reaction equilibria are obtained from a least-squares analysis of the data. The existence of two new zinc(II) ion complexes is reported for the first time: Zn(OH)<sub>2</sub>(HPO<sub>4</sub>)<sup>=</sup> and Zn(OH)<sub>3</sub>(H<sub>2</sub>PO<sub>4</sub>)<sup>=</sup>. A summary of thermochemical properties for species in the systems ZnO-H<sub>2</sub>O and ZnO-Na<sub>2</sub>O-P<sub>2</sub>O<sub>5</sub>-H<sub>2</sub>O is also provided.

#### ACKNOWLEDGEMENT

H. J. Schermerhorn prepared the ZnO used in this study;  
A. N. Lord performed all X-ray diffraction analyses.

## Zinc(II) Oxide Solubility and Phase Behavior in Aqueous Sodium Phosphate Solutions at Elevated Temperatures

S.E. Ziemniak, M.E. Jones, K.E.S. Combs

### INTRODUCTION

Zinc is an alloying constituent of many brass and bronze components used throughout the water-steam circuit of power plants. In order to quantify the hydrothermal aspects of the zinc oxide corrosion products that are transported in such systems, *a priori* knowledge of zinc oxide solubility and phase behavior must be available.

Many solubility studies of ZnO have been performed in alkaline media at room temperature, cf. summaries provided by Baes and Mesmer<sup>(1)</sup> or Khodakovskii and Elkin<sup>(2)</sup>, so that reliable standard free energies of formation are available for the series of hydroxocomplexes  $Zn(OH)_n^{(2-n)}$  ( $n = 2, 3, 4$ ). An additional high-temperature ZnO solubility study was performed in pure water and aqueous sodium hydroxide<sup>(2)</sup>, so that a fairly reliable solubility data base exists over a broad range of alkalinity and temperature.

With regard to solid phase stability in the ZnO-H<sub>2</sub>O system, ZnO is known to be thermodynamically stable relative to  $\epsilon$ -Zn(OH)<sub>2</sub> at 298 K. However, the hydrous oxide form is known to resist transformation for times long enough to permit accurate solubility measurements at room temperature<sup>(3)</sup>. As phosphate concentration and temperature increase, phosphate ion complexes of the hydrolyzed zinc(II) ion are expected to dominate over the usual zinc(II) ion hydroxocomplexes present in solution. In alkaline sodium phosphate solutions, this situation eventually leads to the precipitation of a sodium salt of the phosphato-hydroxo-zincate ion. Under these circumstances, ZnO is no longer

the stable solid phase. Thilo and Schulz<sup>(4)</sup> have already characterized  $\text{NaZnPO}_4 \cdot \text{H}_2\text{O}$  as the stable sodium ion salt precipitated from aqueous  $\text{Na}_2\text{HPO}_4$  solutions at ambient temperatures. Dehydration to  $\text{NaZnPO}_4$  is expected at higher temperatures<sup>(4,5)</sup>.

The present work was undertaken to establish the experimental and theoretical bases for determining solubilities (and stabilities) of a zinc oxide corrosion product ( $\text{ZnO}$ ) in aqueous sodium phosphate solutions at elevated temperatures. Our method involved pumping sodium orthophosphate solutions of known compositions through a  $\text{ZnO}$  bed and analyzing the emerging solution for Zn. Based on these solubility measurements, thermochemical properties were established for the following  $\text{Zn(II)}$  anionic complexes:  $\text{Zn(OH)}_2\text{(aq)}$ ,  $\text{Zn(OH)}_3^-$ ,  $\text{Zn(OH)}_4^{=}$ ,  $\text{Zn(OH)}_2(\text{HPO}_4)^{=}$ , and  $\text{Zn(OH)}_3(\text{H}_2\text{PO}_4)^{=}$ . Similar properties were also established for  $\text{NaZnPO}_4$  based on a thermodynamic analysis of the  $\text{ZnO}/\text{NaZnPO}_4$  solid phase transformation reaction equilibrium.

## EXPERIMENTAL

### Materials

Zinc oxide was prepared from "Baker Analyzed" reagent grade zinc oxide powder supplied by the J. T. Baker Chemical Company. Because the as-received powder was too fine to be retained as a packed column in a flowing autoclave system, it was transformed into larger particles by compaction followed by attrition through a 10 mesh sieve onto a 20 mesh sieve. The particles were then fired at 1473 K for 16 hr in an air atmosphere and slowly cooled to room temperature. The material produced in this manner consisted of hard, irregular-shaped, pale yellow particles with dimensions of 1.3 to 2.5 mm. The color change from white to yellow during and after sintering is a naturally

occurring phenomenon related to a thermal shift in the electron energy absorption band to the visible region. No chemical change in the composition of zinc oxide is produced by this phenomenon.

X-ray diffraction analysis confirmed the presence of a single phase hexagonal lattice structure characteristic of zinc oxide ( $a = 3.2503 \pm 0.0003 \text{ \AA}$  and  $c = 5.2064 \pm 0.0005 \text{ \AA}$ ). Emission spectroscopy found iron to be the major impurity: 60 ppm.

Deionized, deoxygenated water (obtained from Vapodur 607 and Amberlite IRN-150 ion-exchange resin columns) was used throughout the experimental program. This water had a resistivity  $>1 \text{ Mohm-cm}$  and contained  $<0.1 \text{ mg-L}^{-1}$  silica. Linde commercial grade nitrogen was used to sparge dissolved oxygen to values  $<0.005 \text{ mg-L}^{-1}$ . Test solutions were prepared volumetrically in the feed tanks using reagent grade sodium phosphate.

After completing the final solubility run (at high temperature), flow through the solubility apparatus was terminated. The zinc oxide charge was then removed and subjected to additional characterization. Digestion in acid, followed by quantitative wet chemistry analyses revealed a Zn/Na/P atom ratio of 200/1/1. Elemental microanalyses of fractured ZnO particles, performed via the energy dispersive X-ray (EDX) attachment to a scanning electron microscope, revealed significant P/Zn ratios (~0.6) at the surface edges. However, the ZnO particle interiors were free of phosphate. Repeat X-ray diffraction analyses (of powdered material) revealed no changes in ZnO lattice parameters, although trace amounts of an additional phase, presumed to be  $\text{NaZnPO}_4$ , were also detected. The ZnO surface deposits were solubilized by a brief, room-temperature soak in dilute hydrochloric acid; analyses of the supernatant

liquid gave Na/P = 1. The above analyses indicate that a NaZnPO<sub>4</sub> coating formed on the ZnO surfaces during exposure in the solubility apparatus.

### Apparatus

The solubility measurements were made using two identical flowing autoclave systems. A diagram of an individual system is shown in Figure 1. Although each system was constructed using stainless steel components, all high-temperature portions as well as the sampling lines were platinum-lined. Further details on the construction and operation of the apparatus are contained in Reference (6). The experimental program consisted of solubility measurements conducted in deoxygenated water maintained with a one atmosphere blanket of nitrogen cover gas. Feedwater compositions are shown in Table I.

TABLE I. Feedwater Compositions

Run	Phosphate, mmol/kg	Na/P, molar	pH at 298 K	Conductivity μS-cm <sup>-1</sup>
1	0.551 ± 0.016	2.300 ± 0.011	10.24 ± 0.03	150 ± 3
2	1.658 ± 0.032	2.334 ± 0.005	10.68 ± 0.05	438 ± 8
3	3.327 ± 0.042	2.328 ± 0.007	11.02 ± 0.01	805 ± 18
4	10.95 ± 0.32	2.349 ± 0.006	11.29 ± 0.02	2375 ± 20
5	53.07 ± 0.63	2.346 ± 0.013	11.38 ± 0.02	8375 ± 80
6	10.64 ± 0.11	2.176 ± 0.003	10.98 ± 0.03	2090 ± 50
7	10.64 ± 0.11	2.810 ± 0.008	11.70 ± 0.02	3090 ± 70

### Procedures

After the system was stabilized at a desired temperature, steady-state conditions were maintained for at least 60 min; the system flow was then diverted into the sampling system. Each sample, consisting of ~240 mL of solution, was collected in a polyethylene bottle containing 0.25 mL of redistilled concentrated nitric acid. Triplicate samples were withdrawn at each temperature. After the three samples had been collected, the temperature

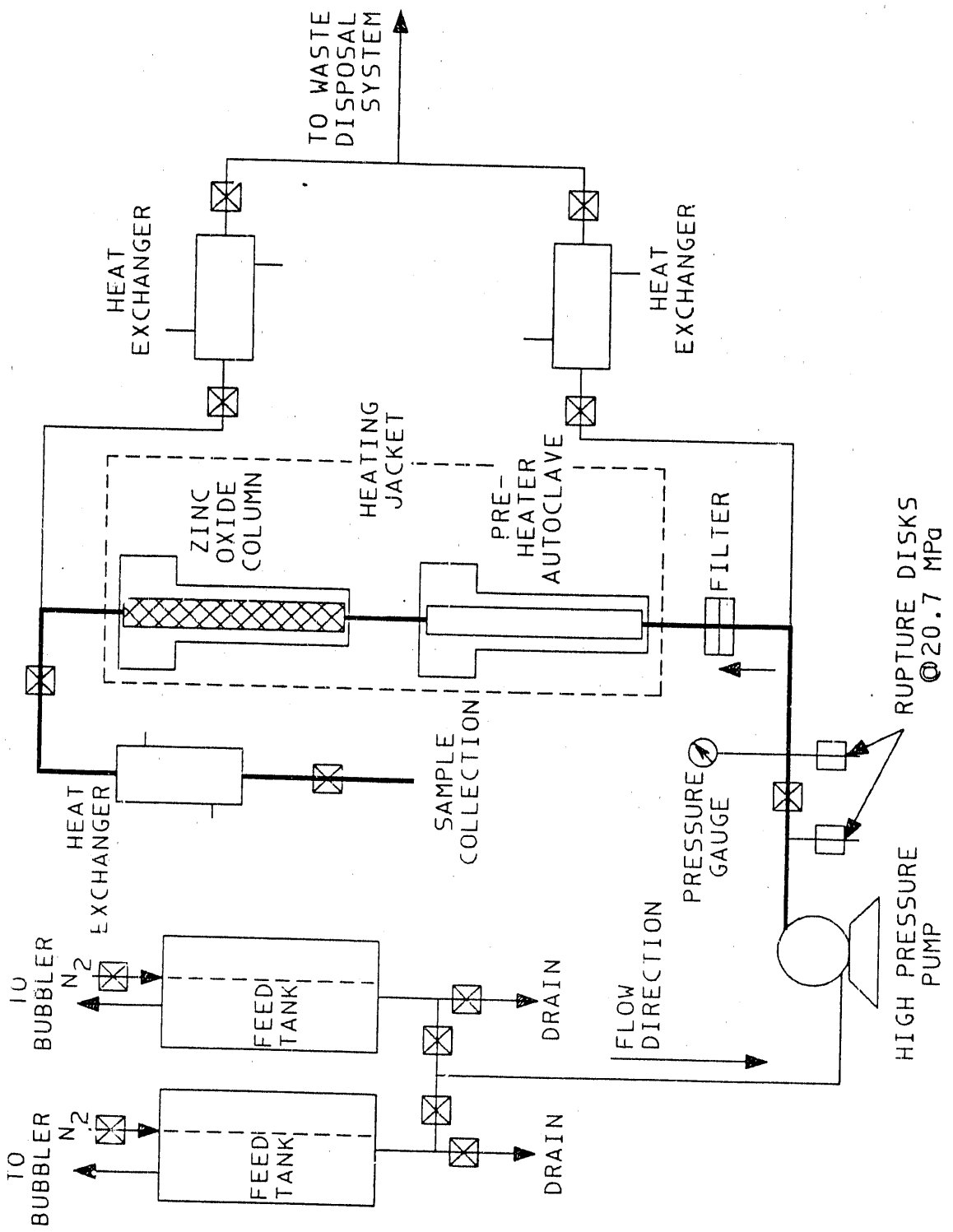


Figure 1. Schematic of Flowing Autoclave System used in Zinc(II) Oxide Solubility Investigation.

controller and Variac settings were changed to establish a new temperature. From 30 to 90 min were required to stabilize the system at the new temperature. After an additional 60 min or longer, the sampling procedure was repeated. This process of changing temperature, allowing time for equilibration, and sampling, continued throughout each experimental run.

Each sample was weighed and then concentrated to a volume of 10.0 mL in a Pyrex beaker. The resulting solution was analyzed for zinc by atomic absorption, utilizing standard techniques. A Perkin-Elmer Model 303 Atomic Absorption Spectrophotometer was used with an air-acetylene flame. A set of sodium phosphate solutions containing known amounts of zinc was run several times with each group of samples analyzed. Phosphate concentrations and sodium-to-phosphate molar ratios were determined by potentiometric titration with dilute hydrochloric acid.

The actual experimental program consisted of seven runs (see Table I) during which the nominal temperature range 294 to 560 K was covered. The first two runs traversed the temperature range in three intervals: (1) increasing from 294 to 408 K in 14 K increments, (2) decreasing from 533 to 422 in 28 K increments, and (3) increasing from 408 to 560 K in 28 K increments.

In Runs 3 to 7 a transformation of the zinc oxide bed occurred at higher temperatures. This transformation was manifested by decreases in zinc solubilities with time (at temperature) and by changes in the composition of the effluent sodium phosphate solutions. Representative data, as presented in Table II, confirmed that the bed transformation was associated with the formation of a layer of  $\text{NaZnPO}_4$  (i.e.,  $\text{Na}/\text{P} = 1.0$ ) on the  $\text{ZnO}$  surface. Therefore, the sequence of subsequent sampling/operating events became very important,

TABLE III. ZnO Bed Transformation Effects

Run No.	Operational Change	Result			
		Phosphate, $\mu\text{mol/kg}$	Na/P	Zn Solubility, $\mu\text{mol/kg}$	
3P	Temperature Increase (380 + 491 K)	Influent: Effluent:	3.233 2.664 2.896 2.969 2.969	2.318 2.402 (4 hrs) 2.450 (23 hrs) 2.424 (47 hrs) 2.431 (73 hrs)	15.695 8.138 7.358 7.022
4P	Temperature Increase (407 + 423 K)	Influent: Effluent:	10.951 10.003	2.321 2.432	Na/P Loss = 1.1
6P	Temperature Increase (292 + 310 K)	Influent: Effluent:	10.635 10.845	2.176 2.154	Na/P Loss = 1.1
7P	Temperature Increase (292 + 311 K)	Influent: Effluent:	10.635 10.845	2.810 2.775	Na/P Gain = 1.0
7P	Temperature Increase (464 + 477 K)	Influent: Effluent:	10.635 8.687	2.810 3.224	Na/P Loss = 1.0

because it was necessary to ensure that zinc solubilities were being measured for the thermodynamically stable solid phase at operating conditions (i.e.,  $\text{NaZnPO}_4$ ). Run 3 omitted the first  $\Delta T$  interval and Runs 4 to 7 were conducted by increasing temperature from 380 to 560 K in 14 K increments. Additional (replicate) samples were withdrawn at 477, 455, and 408 K at the end of Runs 6 and 7.

## RESULTS

### Solubility Data

Results from the experimental program, in terms of measured zinc solubilities as a function of temperature, are presented in Table III. The elemental zinc concentrations represent averages of triplicate samples taken  $\sim \frac{1}{2}$  hr apart and are given in micromolality units,  $\mu\text{M}$  ( $\mu\text{mol}$  per kilogram of water). The small amounts of material lost in the sampling line have been neglected. The temperature value listed for a particular sample was the average of the two downstream thermocouple readings at the start and completion of sampling.

Consistent with our previous discussion, the zinc solubilities reported in Table III include only those values unaffected by bed transformation effects.

### Thermodynamic Analysis

Zinc oxide is expected to solubilize in aqueous solutions via the following reaction:

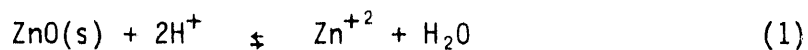
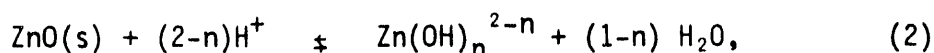


TABLE III. Measured  $ZnO/NaZnPO_4$  Solubilities in Aqueous Sodium Phosphate Solutions

Run 1		Run 2		Run 3		Run 4	
<u>T(K)</u>	<u>Zn*</u>	<u>T(K)</u>	<u>Zn*</u>	<u>T(K)</u>	<u>Zn*</u>	<u>T(K)</u>	<u>Zn*</u>
339.3	0.769	338.7	1.348				
352.0	0.909	352.6	1.606				
368.2	1.074	367.0	1.805				
379.8	1.201	379.3	2.035				
394.3	1.391	395.4	2.295				
407.6	1.637	407.6	2.555				
407.6	1.759	408.2	2.539				
423.7	2.096	424.8	2.998				
435.9	2.310	434.3	3.243			436.5	6.563
449.3	2.493	449.3	3.763			449.3	4.803
463.7	2.769	463.2	4.375			463.7	4.436
479.3	2.968	478.7	4.911	449.3	5.538	477.6	4.222
491.5	3.167	489.8	5.125	478.7	5.568	490.9	4.176
505.9	3.304	504.8	5.813	504.8	5.308	504.8	3.901
519.3	3.503	519.8	6.150	518.2	4.819	519.3	3.901
533.2	3.549	533.2	6.578	531.5	4.895	532.0	3.595
546.5	3.778	546.5	6.884	547.0	4.314	547.0	3.488
561.5	3.824	560.9	7.404	563.7	3.641	561.5	3.121
Run 5		Run 6		Run 7			
<u>T(K)</u>	<u>Zn*</u>	<u>T(K)</u>	<u>Zn*</u>	<u>T(K)</u>	<u>Zn*</u>		
		396.5	4.3				
		408.2	3.02				
		408.2	3.503	394.3	23.94		
379.8	18.40	408.2	3.335	408.7	21.20		
394.8	16.29	420.9	3.014	408.7	21.68		
408.2	13.60	435.9	2.662	408.7	22.23		
408.7	14.23	449.8	2.448	410.4	22.64		
422.0	11.36	455.9	2.356	420.4	19.67		
434.8	11.14	463.7	2.555	436.5	17.36		
449.3	9.683	475.9	2.341	455.4	13.94		
463.2	8.857	477.0	2.249	473.7	11.32		
478.2	8.092	477.6	2.555	474.3	11.20		
491.5	7.557	491.5	2.432	490.9	9.974		
506.5	7.220	505.9	2.493	505.4	8.460		
519.8	7.022	519.8	2.616	519.3	7.542		
532.6	6.593	533.2	2.371	533.7	6.593		
547.6	6.287	547.0	2.279	546.5	5.859		
561.5	5.966	560.4	2.111	560.4	5.155		

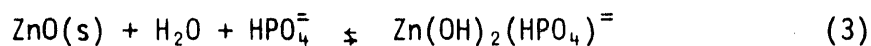
\* Units:  $10^{-6}$  mol/kg

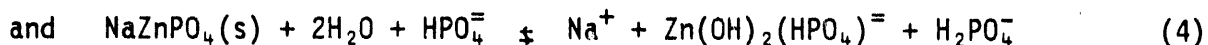
Furthermore, the dissolved zinc(II) ion is known to be stabilized in aqueous solutions by the formation of aquo and hydroxocomplexes. That is, the divalent zinc ion becomes surrounded by an inner hydration sheath of six water molecules with octahedral symmetry<sup>(7)</sup>. Stepwise dissociation of these complexed water molecules occurs as the pH of the solution is elevated. Thus, the overall zinc oxide dissolution reaction becomes the following sequence:



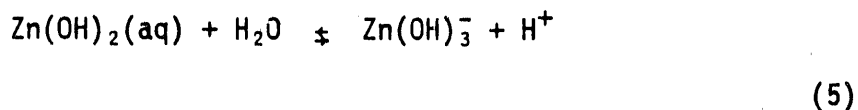
where n refers to the state of hydrolysis and may take on the values 0, 1, 2, 3, or 4. Due to the characteristic hydrolysis behavior of the zinc(II) ion, (cf. Reference 1) and the alkaline pH range employed during the present study, concentrations of the species corresponding to n = 0 and 1 are expected to contribute insignificantly to the zinc oxide solubility database.

On the other hand, if the high-temperature portions of Runs 3 to 7 indeed represent an equilibrium with another solid phase in the system ZnO-Na<sub>2</sub>O-P<sub>2</sub>O<sub>5</sub>-H<sub>2</sub>O, then a dissolution reaction involving the NaZnPO<sub>4</sub> solid is required. Recall also that various Zn(II) phosphatocomplex forms are possible in aqueous phosphate solutions. The following phosphato complexes of the unhydrolyzed zinc(II) ion have been reported: Zn(HPO<sub>4</sub>)<sup>(8)</sup> and Zn(H<sub>2</sub>PO<sub>4</sub>)<sup>+(9)</sup>; similar complexes involving hydrolyzed, divalent zinc ions are possible, although information concerning these equilibria is not yet available. By similarity to the reported solubility behavior of copper(II) oxide in aqueous sodium phosphate<sup>(10)</sup>, we may expect significant concentrations of Zn(OH)<sub>2</sub>(HPO<sub>4</sub>)<sup>=</sup> to be present. Therefore, the suggested dissolution reactions are:

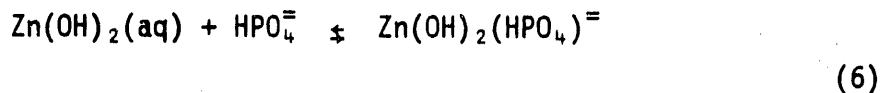




The concentrations of each possible zinc(II) ion complex were then calculated in terms of an equilibrium constant for either a stepwise hydrolysis reaction, i.e.:



or a phosphatocomplexing reaction, i.e.:



The thermodynamic relationships

$$-RT \ln K = \Delta G = \Delta H - T \Delta S \quad (7)$$

were introduced at this point to allow calculation of all zinc(II) ion complex concentrations as functions of temperature. The total molality of zinc in solution was then calculable by summation over the mononuclear zinc(II) species present. Where possible, a three parameter model was used to describe  $\Delta G$  as a function of temperature. This approximation assumes that the difference in heat capacities between reactants and products for each reaction is a constant (C). Integration of the applicable thermodynamic relationships gives

$$\Delta H = A + CT \text{ and } \Delta S = B + C \ln T, \quad (8)$$

where A, B, and C are fitted constants.

To evaluate the experimental solubilities of Table III in terms of concentrations of the possible complexed/hydrolyzed zinc species present required that the pH (hydronium ion concentration) be known at the existing solution conditions. This quantity depended on the sodium phosphate molality, as well as the orthophosphate ion and water dissociation constants. These parameters, which are functions of solution temperature, are defined below and tabulated in Table IV.

$$K_w = [H^+][OH^-] \quad (9)$$

$$Q_1 = \frac{[H_2PO_4^-]}{[H_3PO_4][OH^-]} \quad (10)$$

$$Q_2 = \frac{[HPO_4^{2-}]}{[H_2PO_4^-][OH^-]} \quad (10a)$$

$$Q_3 = \frac{[PO_4^{3-}]}{[HPO_4^{2-}][OH^-]} \quad (10b)$$

$$\text{with } \log K = \frac{A}{T} + B + C \ln T + \frac{E}{T^2} \quad (11)$$

Deviations from ideal solution behavior were accounted for by distinguishing between ionic concentration and thermodynamic activity:

$$a_i = \gamma_i C_i \quad (12)$$

where  $a_i$  is the thermodynamic activity,  $\gamma_i$  the ionic activity and  $C_i$  is the ionic concentration. Generally, it was assumed that ionic activity coefficients could be related to ionic strength by an extended Debye-Hückel expression<sup>(14)</sup>:

$$\log \gamma_i = \frac{-SZ_i^2 \sqrt{I}}{1 + 1.5 \sqrt{I}} \quad (13)$$

where  $S$  is the limiting Debye-Hückel slope ( $\approx 0.51$  at  $298\text{ K}$ )<sup>(11)</sup>,  $Z_i$  is the ionic charge number, and  $I$  is the ionic strength  $= \sum \frac{1}{2} C_i Z_i^2$ . Dissociation constants  $K_w$ ,  $Q_1$ , and  $Q_2$  were corrected for ionic strength via literature correlations<sup>(11) and (12)</sup>.  $K_w$  was corrected to a pressure of  $8.97\text{ MPa}$  using the correlation presented in Reference 11.

TABLE IV. Dissociation Behavior of Selected Compounds

Compound Undergoing Dissociation	A	B	C	D	E	Reference Cited
$\text{H}_2\text{O}$	31,286.0	-606.522	94.9734	-0.097611	-2,170,870	Sweeton, Mesmer and Baes <sup>(11)</sup>
$\text{H}_3\text{PO}_4$	17,655.8	-253.198	39.4277	-0.0325405	-810,134	Mesmer and Baes <sup>(12)</sup>
$\text{H}_2\text{PO}_4^-$	17,156.9	-246.045	37.7345	-0.0322082	-897,579	Mesmer and Baes <sup>(12)</sup>
$\text{HPO}_4^{\pm}$	-106.51	7.1340	-	-0.017459	-	Treloar <sup>(13)</sup>

An overall neutrality balance was finally used to determine  $[\text{H}^+]$  for each data point. For the most general case, the balance is:

$$\sum_{n=3}^4 (2-n) [\text{Zn(OH)}_n^{(2-n)+}] + \sum_{k=1}^3 \sum_{m=2}^4 (2-m-k) [\text{Zn(OH)}_m (\text{H}_2\text{PO}_4)_k^{(2-m-k)+}]$$

$$+ \sum_{i=1}^3 \sum_{p=2}^4 (2-p-2i) [\text{Zn(OH)}_p (\text{HPO}_4)_i^{(2-p-2i)+}] + [\text{Na}^+] + [\text{H}^+] =$$

$$[\text{OH}^-] + 3[\text{PO}_4^{3-}] + 2[\text{HPO}_4^{2-}] + [\text{H}_2\text{PO}_4^-] \quad (14)$$

Since the  $\text{Zn(OH)}_2(\text{HPO}_4)^-$  ion concentration was given in terms of the equilibrium constant for Equation (3) or (4), and the concentrations of the hydrolyzed and complexed Zn(II) species were calculable in terms of equilibrium constants for Equations (5) to (6), the neutrality balance was reduced to an algebraic equation in terms of the unknown,  $[\text{H}^+]$ . To determine how a given scheme of Zn(II) complexes in solution could fit the results, a set of thermodynamic constants was substituted into the neutrality balance (Equation 14), and  $[\text{H}^+]$  concentrations were calculated by a Newton-Raphson iteration procedure. These  $[\text{H}^+]$  values were then used to compute all the soluble zinc species which, after being summed, could be compared with the measured Zn solubilities. The differences were then minimized via a generalized, nonlinear, least-squares curve-fitting routine based on Marquardt's algorithm<sup>(15)</sup>.

When the solubility data were analyzed, the importance of relative errors (i.e., percentage errors), rather than absolute errors, was accounted for by minimizing differences between the logarithms of the experimental and the predicted solubilities. The thermodynamic functions obtained in this manner were then resubstituted into the neutrality balance, and the two-step process

was repeated. Convergence, i.e., the condition when the calculated thermodynamic functions ceased to change, was attained in a few cycles because the dissolved metal ion concentrations were low and had only a minor influence on changes in solution pH.

Results of the data-fitting procedure are illustrated graphically in Figures 2 through 4. The predominant species were found to be  $\text{Zn}(\text{OH})_2(\text{HPO}_4)^{\pm}$ ,  $\text{Zn}(\text{OH})_3^-$  and  $\text{Zn}(\text{OH})_2(\text{aq})$ ; three parameter fits yielded statistically significant correlations. The presence of two other anionic Zn(II) complexes [ $\text{Zn}(\text{OH})_4^{\pm}$  and  $\text{Zn}(\text{OH})_3(\text{H}_2\text{PO}_4)^{\pm}$ ] were also fitted in a statistically significant manner. Due to their lower concentrations, a two parameter thermodynamic model proved to be sufficient; i.e.,  $\Delta H$  and  $\Delta S$  were taken to be independent of temperature.

Table V presents the thermodynamic quantities fitted to the  $\text{ZnO}$  and  $\text{NaZnPO}_4$  dissolution reactions and the subsequent Zn(II) ion hydrolysis and complexing reactions. This fit resulted in an overall standard deviation between measured and fitted Zn solubilities of 9%.

#### DISCUSSION

##### Zinc Oxide Dissolution into $\text{Zn}(\text{OH})_2(\text{aq})$

Because solution pH, hence the hydrolytic state of the zinc(II) ion, was controlled by the quantity of sodium phosphate added, it was not possible to complex measureable levels of  $\text{Zn}^{+2}$  and  $\text{Zn}(\text{OH})^+$  in the present experimental program.

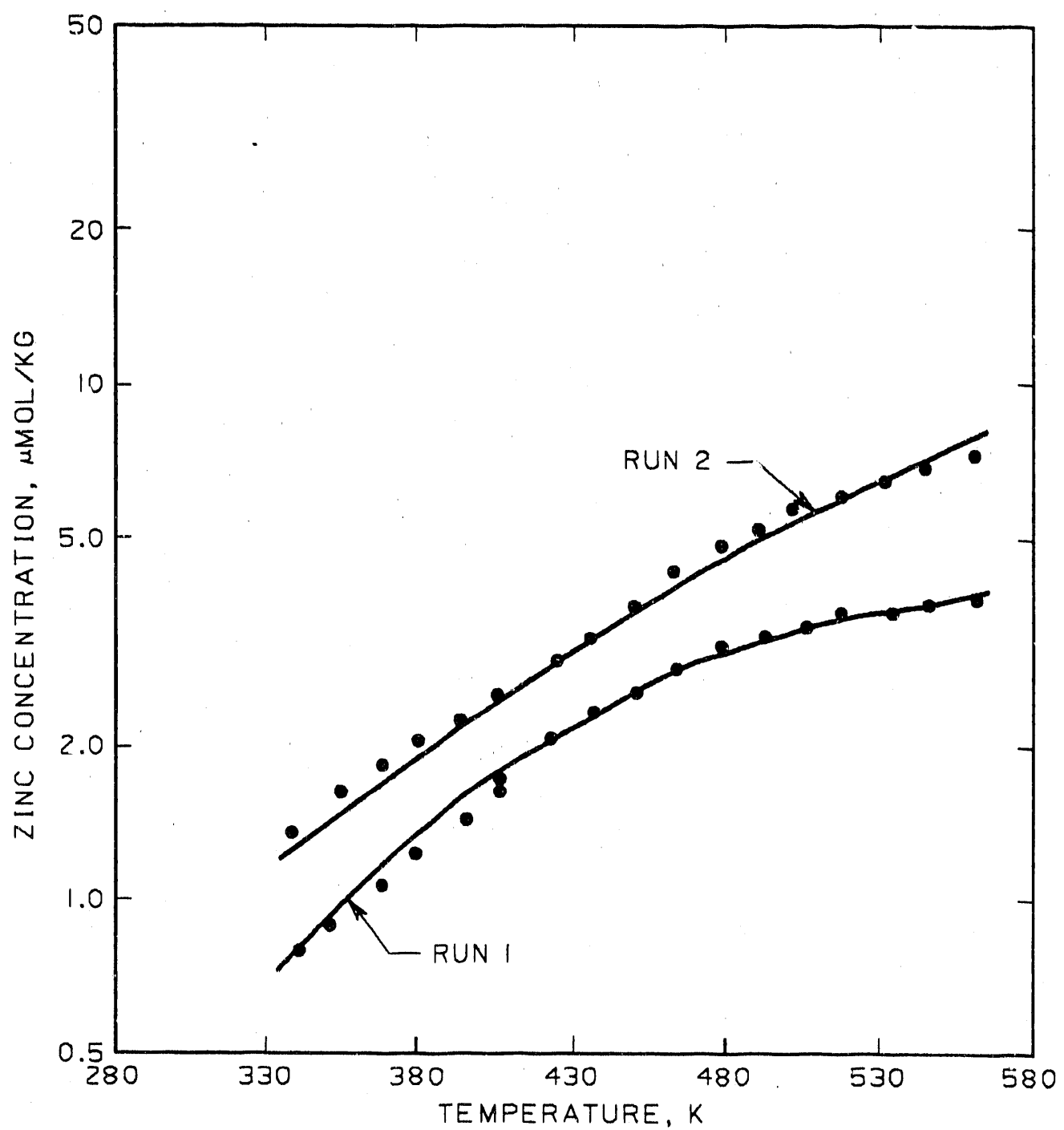


Figure 2. Comparison of Measured and Fitted Solubilities of Zinc Oxide in Sodium Phosphate Solutions (Na/P = 2.3).

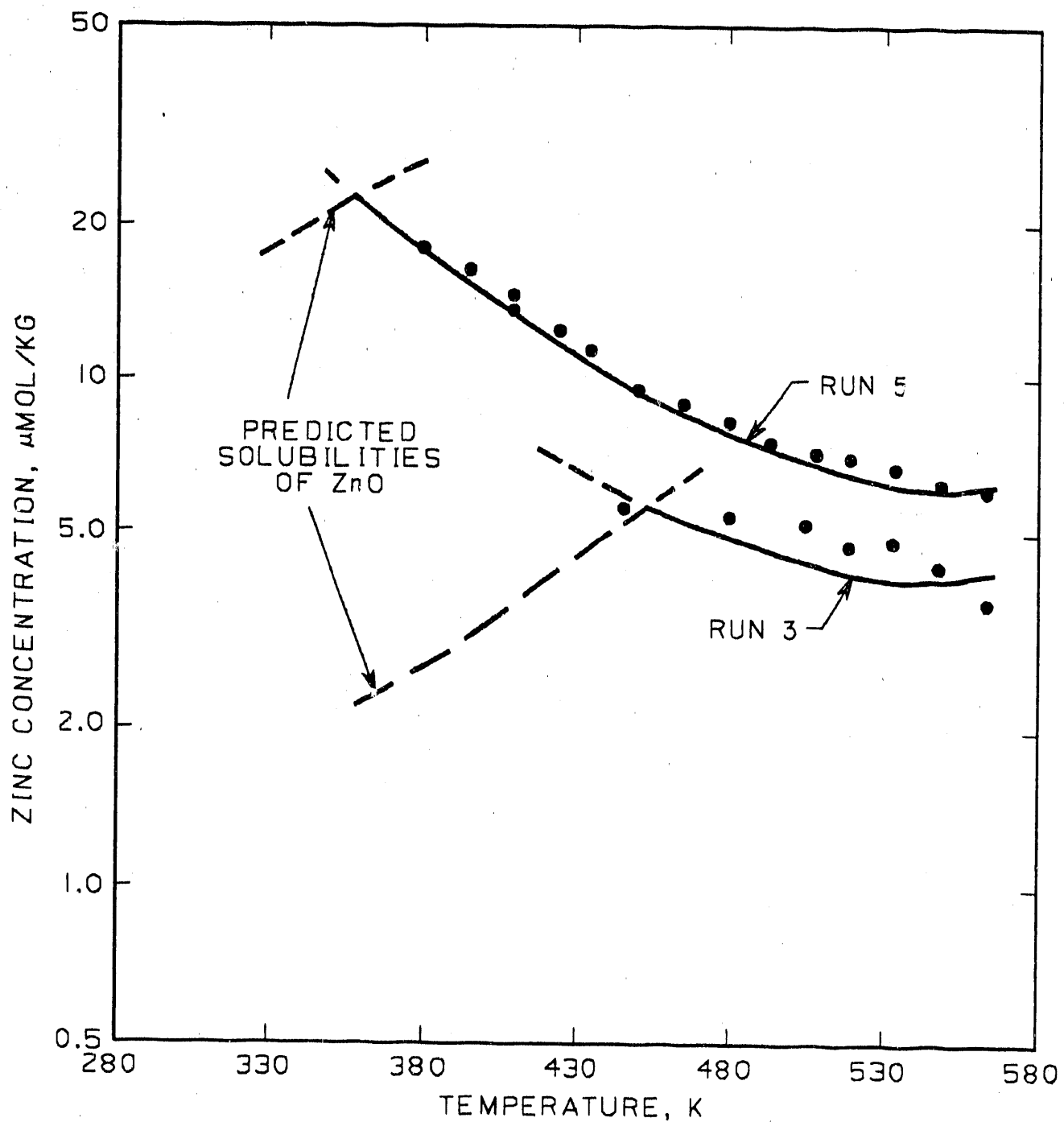


Figure 3. Comparison of Measured and Fitted Solubilities of  $\text{NaZnPO}_4$  in Sodium Phosphate Solutions ( $\text{Na}/\text{P} = 2.3$ ).

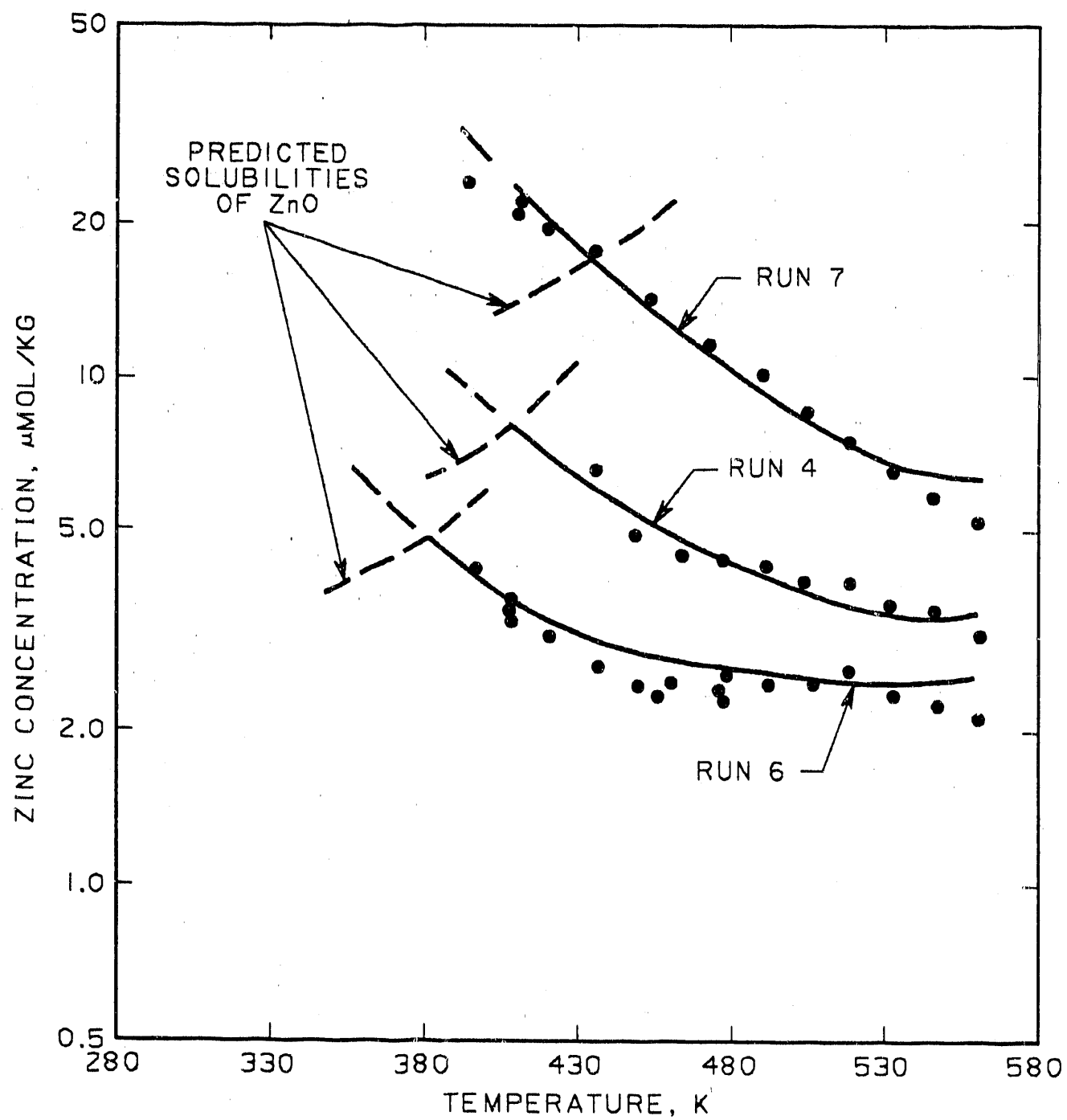


Figure 4. Comparison of Measured and Fitted Solubilities of  $\text{NaZnPO}_4$  in Sodium Phosphate Solutions ( $P = 10.5 \text{ mmol/kg}$ ).

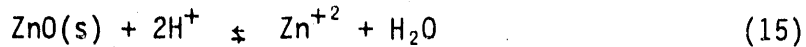
TABLE V. Thermodynamic Equilibria for Calculation of  $ZnO/NaZnPO_4$  Solubilities in Alkaline Sodium Phosphate Solutions via  $\Delta G(T) = A - BT - CT\ln T$ \*

Reaction	$A$ $kJ\cdot mol^{-1}$	$B_1$ $J\cdot mol^{-1}\cdot K^{-1}$	$C_1$ $J\cdot mol^{-1}\cdot K^{-1}$	$\Delta G^\circ(298)$ $kJ\cdot mol^{-1}$
<u>Dissolution</u>				
$ZnO(s) + H_2O + HPO_4^{2-} \rightleftharpoons Zn(OH)_2(HPO_4)^{2-}$	88.73 $\pm$ 6.63	864.75 $\pm$ 164.50	-119.49 $\pm$ 14.90	33.89 $\pm$ 1.30
$NaZnPO_4(s) + 2H_2O + HPO_4^{2-} \rightleftharpoons Na^+ + Zn(OH)_2(HPO_4)^{2-} + H_2PO_4^-$	177.53 $\pm$ 5.50	2030.29 $\pm$ 55.32	-295.86 $\pm$ 7.49	74.80 $\pm$ 1.33
<u>Phosphatocomplexing</u>				
$Zn(OH)_2(aq) + HPO_4^{2-} \rightleftharpoons Zn(OH)_2(HPO_4)^{2-}$	28.69 $\pm$ 6.07	120.59 $\pm$ 53.22	-1.63 $\pm$ 7.22	-4.50 $\pm$ 2.25
$Zn(OH)_3^- + H_2PO_4^- \rightleftharpoons Zn(OH)_3(H_2PO_4)^{2-}$	-55.76 $\pm$ 10.86	-69.97 $\pm$ 30.34	-	-34.90 $\pm$ 2.16
<u>Hydrolysis</u>				
$Zn(OH)_2(aq) + H_2O \rightleftharpoons Zn(OH)_3^- + H^+$	27.26 $\pm$ 3.45	-105.79 $\pm$ 8.20	-	53.80 $\pm$ 1.11
$Zn(OH)_3^- + H_2O \rightleftharpoons Zn(OH)_4^{2-} + H^+$	19.72 $\pm$ 13.35	-163.44 $\pm$ 31.24	-	68.45 $\pm$ 4.43
$[Zn(OH)_3^- + H_2O \rightleftharpoons Zn(OH)_4^{2-} + H^+]$ **	30.22 $\pm$ 5.07	-141.22 $\pm$ 12.14	-	72.32 $\pm$ 1.55

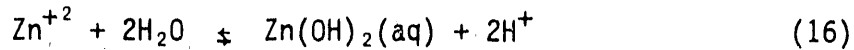
\* All reported uncertainties correspond to one standard deviation.

\*\* Refit including 18 data points from Reference (2), see DISCUSSION.

The standard free energy change for zinc oxide dissolution into the lowest zinc(II) hydrolytic state,  $\text{Zn(OH)}_2\text{(aq)}$ , was determined from Table V to be  $38.16 \pm 3.56 \text{ kJ/mol}$ . This result indicates a  $\text{Zn(OH)}_2\text{(aq)}$  solubility of  $0.2 \mu\text{m}$  at room temperature. A "literature" value for comparison purposes may be obtained by combining standard free energy changes reported for



and



Schindler et al<sup>(16)</sup> have measured  $-63.58 \pm 0.18 \text{ kJ}$  for Equation (15), while Baes and Mesmer<sup>(1)</sup> recommend  $96.44 \pm ?\text{kJ}$  for Equation (16), but state that a higher value would be expected. These values combine to give the Equation (2) equilibrium for  $n = 2$  as  $\Delta G^\circ(298) = 32.86 \text{ kJ}$ . This estimate indicates a  $\text{Zn(OH)}_2\text{(aq)}$  solubility of  $1.75 \mu\text{m}$ , which is clearly too high compared with our  $\text{ZnO}$  solubility measurements (see Figure 2).

Free energy changes for zinc oxide dissolution at elevated temperatures, as determined from a combination of equilibria summarized in Table V, are plotted in Figure 5. The results of Khodakovskii and Elkin<sup>(2)</sup>, obtained at temperatures between 373 and 473 K, are seen to be higher by a maximum of 5 kJ at 473 K. Given an estimated uncertainty of  $\pm 2.9 \text{ kJ}$  for our experimental results at 473 K, the difference is not statistically significant. Note that the lowest  $\text{ZnO}$  solubility value reported by Khodakovskii and Elkin at 373 K ( $1.8 \mu\text{m}$ ) is also consistent with our higher  $\Delta G^\circ(298)$  estimate, because most of the soluble Zn(II) was present as  $\text{Zn(OH)}_3^-$  rather than  $\text{Zn(OH)}_2\text{(aq)}$ .

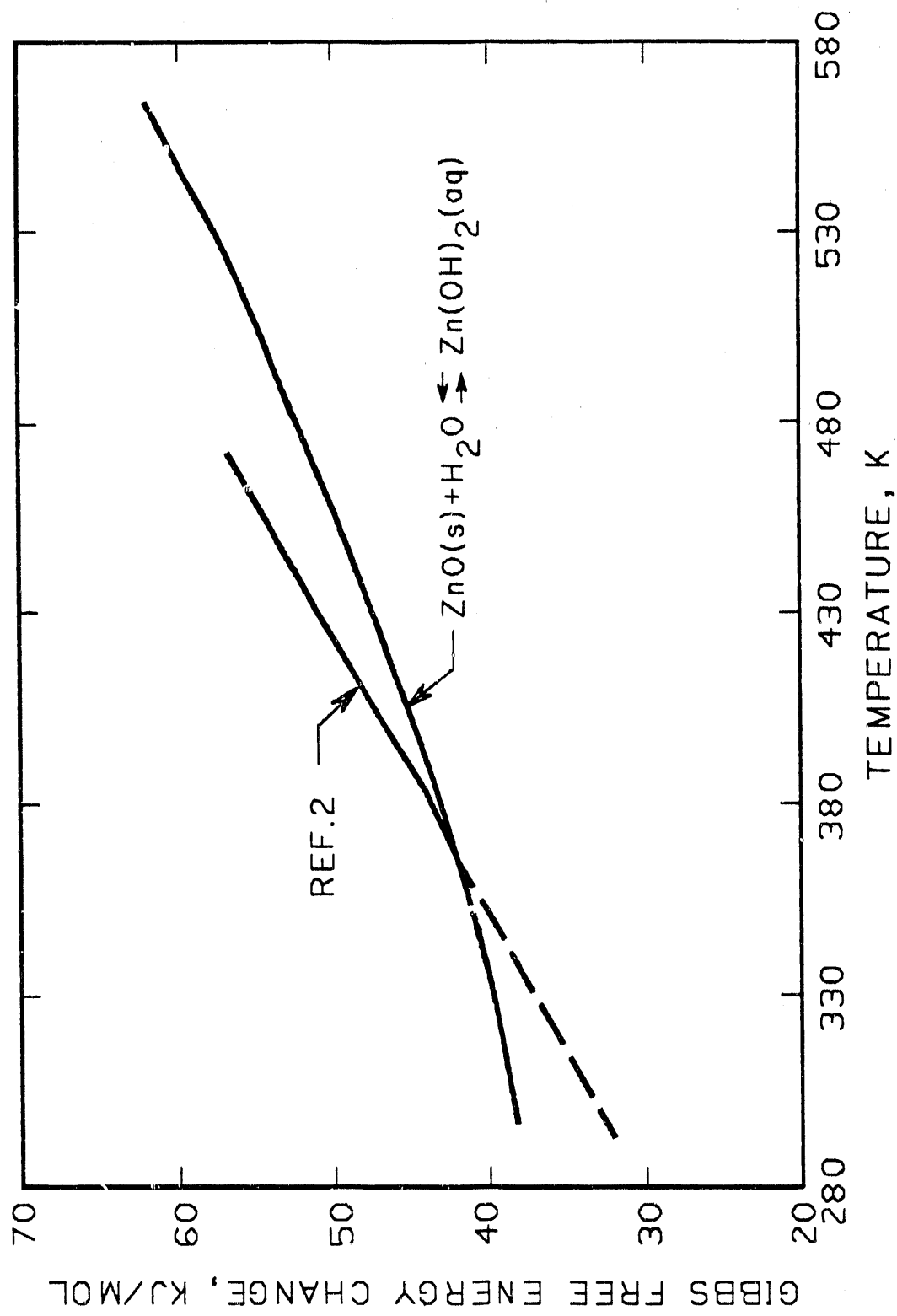


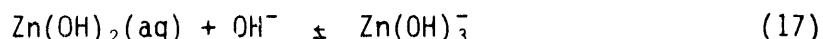
Figure 5. Free Energy Changes Measured During Zinc Oxide Dissolution.

The above discussion is consistent with an equilibrium that exhibits a nonlinear  $\Delta G(T)$  behavior. On the basis of the fitted  $\Delta C_p^{\circ}(298)$  for the ZnO dissolution reaction (-117.9 J/K) and tabulated standard heat capacities (see Table VI), the standard heat capacity for the  $\text{Zn}(\text{OH})_2(\text{aq})$  hydroxocomplex is calculated to be -2.3 J/K.

### Zn(II) Ion Hydrolysis

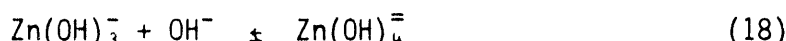
Standard free energy changes for the third and fourth stepwise hydrolysis reactions of the Zn(II) ion were determined to be  $58.83 \pm 1.11$  and  $68.43 \pm 4.43$  kJ, respectively. A literature value for  $\Delta G^{\circ}(298)$  of the third stepwise hydrolysis reaction, derived via difference between  $\Delta G^{\circ}$  for the triple hydrolysis reaction recommended by Baes and Mesmer<sup>(1)</sup> and our revised  $\Delta G^{\circ}$  estimate for Equation (16), is 60.34 kJ. Similarly, literature values recommended by Baes and Mesmer<sup>(1)</sup> give  $\Delta G^{\circ}(298) = 73.05 \pm 1.14$  kJ for the fourth stepwise hydrolysis reaction. In neither case is the disagreement considered to be statistically significant.

The high-temperature equilibria for the above hydrolysis reactions are shown in Figure 6. These results are compared with the results of Khodakovskii and Elkin<sup>(2)</sup>, who determined these hydrolysis equilibria in terms of reaction with the hydroxyl ion:



$$\Delta G(T) = 15314 - 99.41 T$$

and



$$\Delta G(T) = -17324 + 35.32 T$$

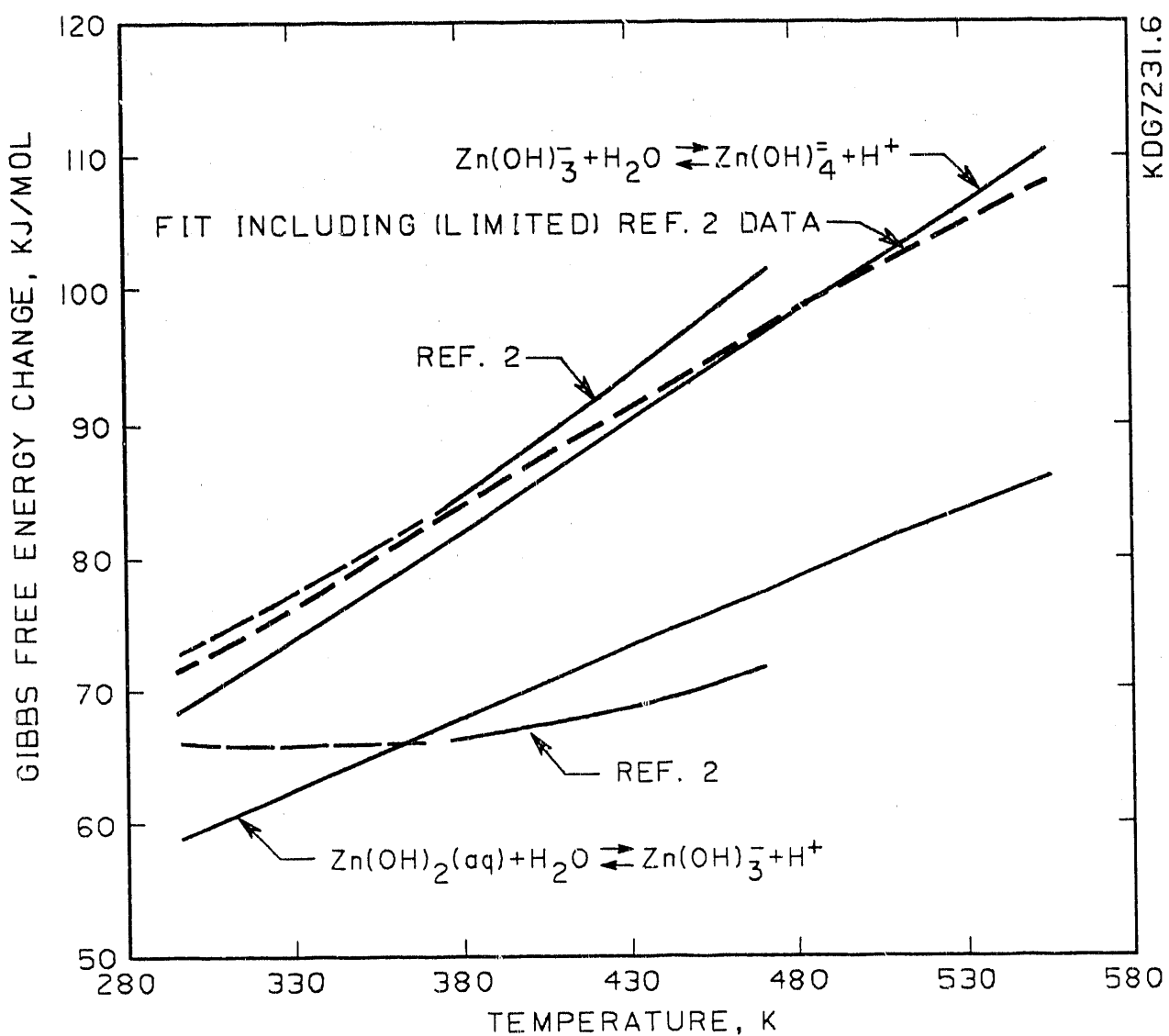


Figure 6. Comparison of Free Energy Changes Associated with Zn(II) Ion Hydrolysis Reactions.

These free energy changes were converted to the form of Equations (5) by adding  $\Delta G_w$ . Results of the two investigations are seen to differ by up to 6 kJ over the temperature range 298 - 473 K.

The source of this discrepancy, with regard to calculation of the third stepwise hydrolysis reaction equilibrium, lies in the analytical methodology selected by Khodakovskii and Elkin<sup>(2)</sup>: an assumed linear  $\Delta G(T)$  dependency fitted to the Equation (17) equilibrium necessarily implies that the corresponding Equation (5) equilibrium will exhibit the nonlinear  $\Delta G(T)$  characteristics shown in Figure 6. This phenomenon is not believed to be real, because subsequent introduction of a heat capacity term into the Equation (5) equilibrium did not yield a meaningful fit.

On the other hand, the limited pH range covered by the present investigation was responsible for relatively imprecise estimates of the fourth stepwise hydrolysis reaction equilibrium. Because higher alkalinitiess were tested by Khodakovskii and Elkin (the pH range 11 through 13 was represented by 18 data points), their estimate of this equilibrium was more precise than ours. Therefore, the above data points were included in our database and a new least-squares fit was performed\*. The new fit is compared with the added data in Figure 7. With the exception of the fourth hydrolysis reaction equilibrium, the modified fit yielded results virtually identical to the original fit. Upgraded thermodynamic parameters for the fourth hydrolysis equilibrium are given in Table V. As shown in Table V and Figure 6, the modified fit

---

\* System pressures at the three temperatures tested were assumed to be 10% above saturation.

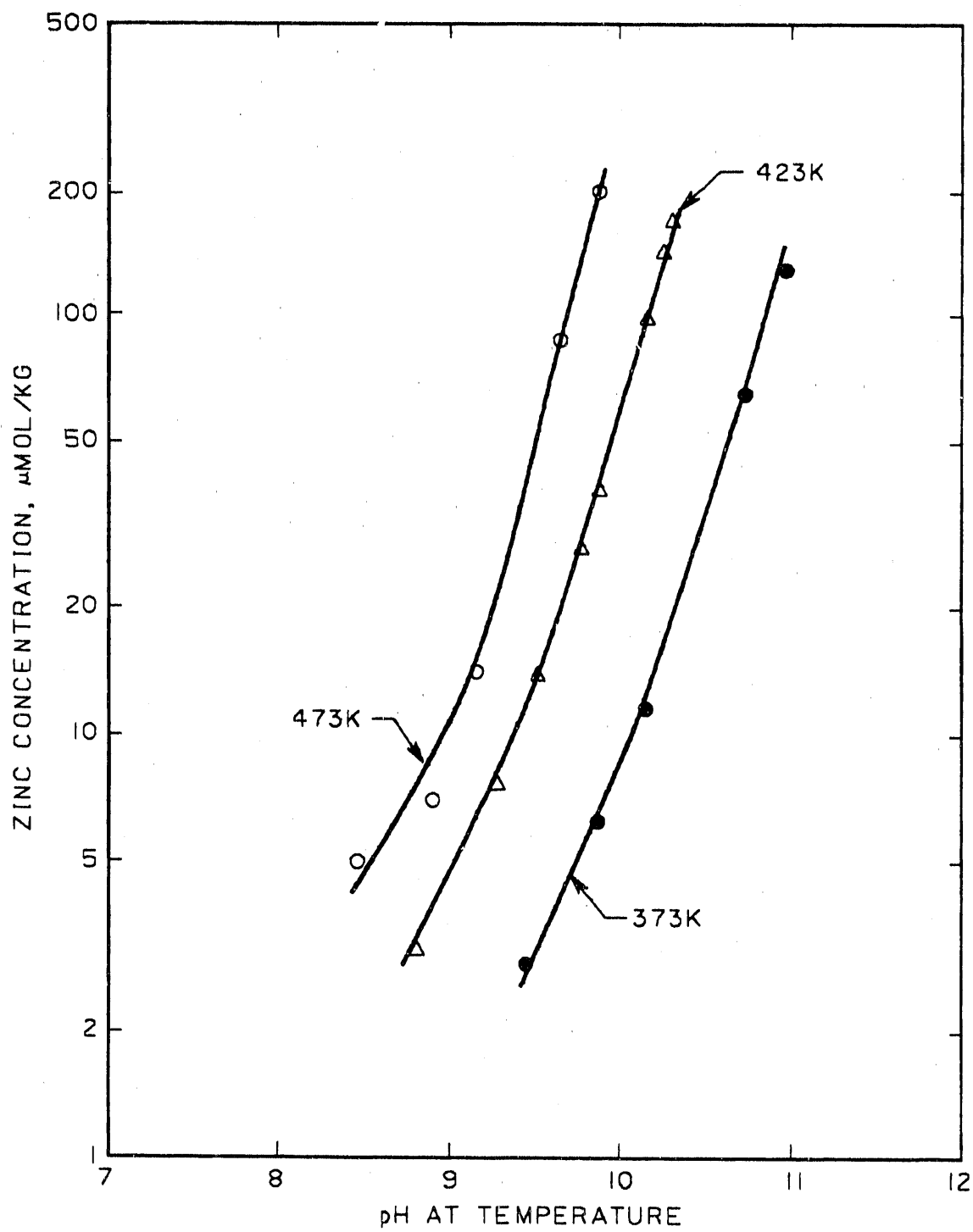


Figure 7. Comparison of Measured and Fitted Solubilities of Zinc Oxide in Sodium Hydroxide Solutions. Data Taken from Khodakovskii and Elkin.<sup>(2)</sup>

increases the precision of the fourth hydrolysis equilibrium and brings about a much closer agreement between the two studies.

By way of closure, Table VI provides a summary of thermochemical properties of species in the ZnO-H<sub>2</sub>O system. Inconsistencies in the literature have led to different recommended properties for Zn(OH)<sup>+</sup> by two independent reviews<sup>(1,2)</sup>. We conclude that the subsequent inclusion of three ZnO solubility measurements in pure water by Khodakovskii and Elkin<sup>(2)</sup> is insufficient to reliably determine two Zn(OH)<sup>+</sup> properties ( $\Delta H_f^\circ$ ,  $S^\circ$ ). However, by assuming that Zn(II) hydrolysis is similar to that for Cu(II), we expect Zn(OH)<sup>+</sup> to exhibit  $\Delta G^\circ(298) \approx 55 \text{ kJ-mol}^{-1}$  for stepwise hydrolysis (similar to <sup>(1)</sup>) and to possess a large, positive ionic entropy (similar to <sup>(2)</sup>).

All ionic entropies for the families of Zn(II) and Cu(II) hydroxo-complexes, therefore, are positive quantities (see Figure 8). Since unhydrolyzed metal ion entropies are negative, hydroxocomplex formation is viewed as a structure-breaking process. This behavior may indicate a change in coordination number of the central metal ion from six to four.

#### ZnO/NaZnPO<sub>4</sub> Transformation

The thermodynamic instability of zinc oxide in concentrated sodium phosphate solutions is explained by the precipitation of a sodium salt of the phosphato-hydroxo-zincate ion. By combining fitted chemical equilibria for the ZnO and NaZnPO<sub>4</sub> dissolution reactions, an equilibrium constant may be derived for the overall transformation reaction:

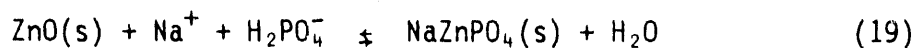


TABLE VI. Thermochemical Parameters for Species in the ZnO-H<sub>2</sub>O System

Species	$C_p^{\circ}(298)$ $\text{J}\cdot\text{mol}^{-1}\cdot\text{K}^{-1}$	$S^{\circ}(298)$ $\text{J}\cdot\text{mol}^{-1}\cdot\text{K}^{-1}$	$\Delta H_f^{\circ}(298)$ $\text{kJ}\cdot\text{mol}^{-1}$	$\Delta G_f^{\circ}(298)$ $\text{kJ}\cdot\text{mol}^{-1}$	Reference Cited
Zn(s)	25.40	$41.63 \pm 0.21$	0	0	17
$\epsilon\text{-Zn(OH)}_2\text{(s)}$	72.4	$76.99 \pm 0.21$	-645.47	$-555.93 \pm 0.21$	2
ZnO(s)	40.25	$43.64 \pm 0.42$	$-350.83 \pm 0.21$	$-320.91 \pm 0.25$	17
H <sub>2</sub> (g)	28.83	$130.58 \pm 0.08$	0	0	17
O <sub>2</sub> (g)	29.37	$205.02 \pm 0.04$	0	0	17
H <sup>+</sup> (aq)	-71	-22.2	0	0	18, 19
H <sub>2</sub> O	75.31	$69.96 \pm 0.08$	$-285.85 \pm 0.04$	$-237.19 \pm 0.04$	17
Zn <sup>+2</sup> (aq)	-164	$-154.8 \pm 1.3$	$-153.64 \pm 0.42$	-147.23	2, 19
Zn(OH) <sup>+</sup> (aq)	-	*	*	$-333.3$ $-342.0$	1 2
Zn(OH) <sub>2</sub> (aq)	-2.3	68.5	-611.74	-519.67	This Work
Zn(OH) <sub>3</sub> <sup>-</sup> (aq)	-	54.9	-870.31	-698.08	This Work
Zn(OH) <sub>4</sub> <sup>2-</sup> (aq)	-	5.8	-1125.96	-862.97	This Work

\* No values are recommended due to widely conflicting results, i.e.,  $S^{\circ}(\text{ZnOH}^+)$  =  $-46.2^{(1)}$  and  $+42.7^{(2)}$   $\text{J}\cdot\text{mol}^{-1}\cdot\text{K}^{-1}$ , see DISCUSSION.

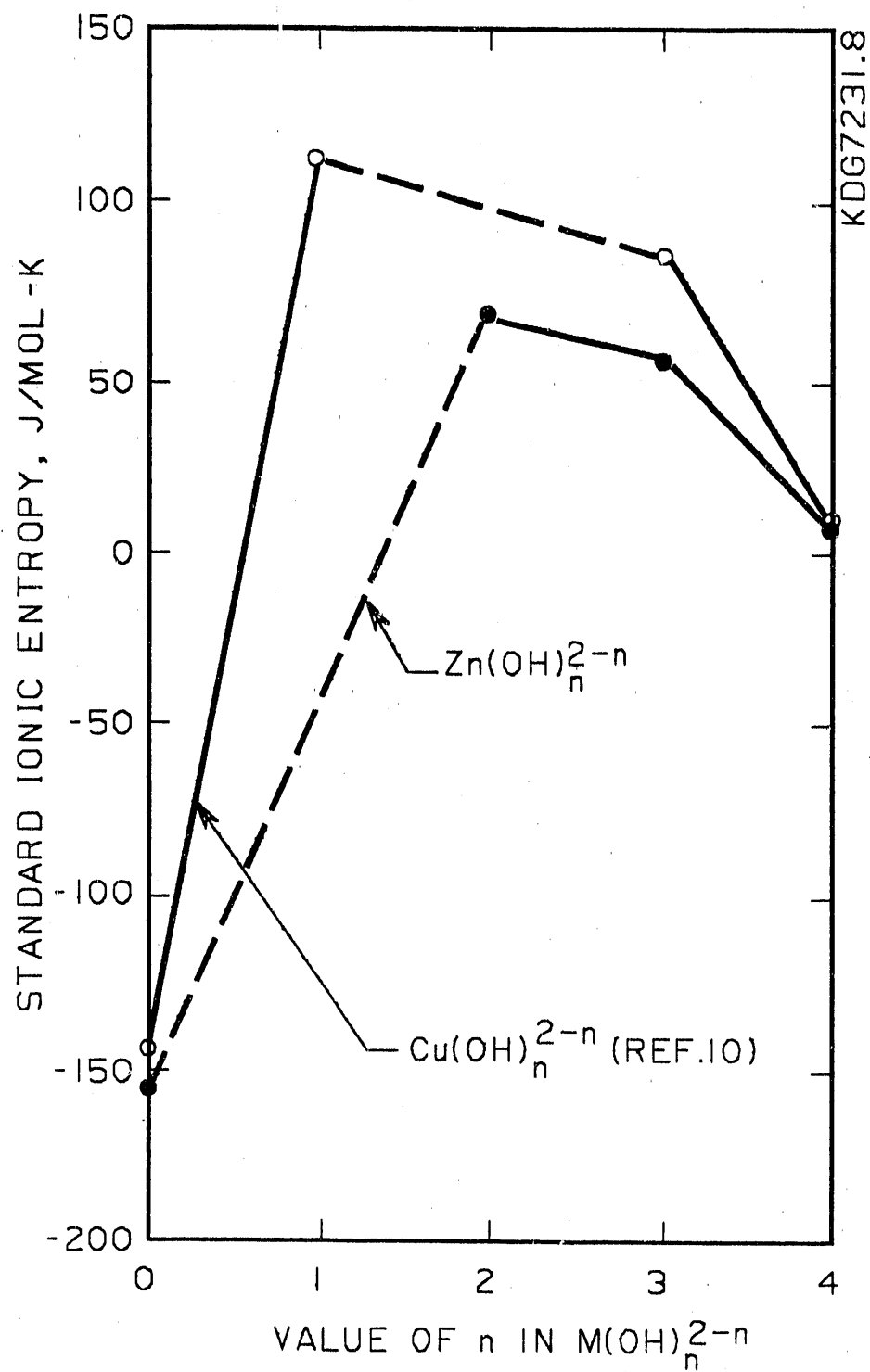


Figure 8. Standard Entropies for Zn(II) and Cu(II) Ions and their Hydroxocomplexes.

where  $\log k_0 = -\log [Na^+][H_2PO_4^-] + \frac{2S\sqrt{I}}{1 + 1.5\sqrt{I}}$  (20)

On the basis of Table V values, it is found that

$$\log k_0 = \frac{4638.9}{T} - 60.886 + 9.213 \ln T.$$

Zinc oxide will remain stable as long as the sodium phosphate concentration product,  $[Na^+][H_2PO_4^-]$ , corrected for nonideal behavior by Equation (13), is less than the  $1/k_0$  value at a given temperature. Conversely, if the phosphate content increases so that  $[Na^+][HPO_4^-] > 1/k_0$ , then  $ZnO$  becomes unstable and will transform to  $NaZnPO_4$ . This equilibrium concept is illustrated in Figure 9.

Another way of viewing this transformation is that the zinc compound with the lowest solubility is the one that precipitates from solution. Zinc oxide is stable at lower temperatures because the solubility limits of  $NaZnPO_4$  are very high. However, at high temperatures  $NaZnPO_4$  becomes sparingly soluble while the  $ZnO$  solubility limits increase greatly. The transformation line (i.e., phase boundary) shown in Figure 9 represents the locus of points at which the zinc solubility limits of the two phases --  $ZnO$  and  $NaZnPO_4$  -- are equal.

#### Zn(II) Ion Phosphatocomplex Formation

The distribution of zinc(II) ion hydrolytic and phosphatocomplex species present in solution at 298 and 560 K is plotted in Figure 10 as a function of sodium phosphate concentration. It is readily seen that  $Zn(OH)_2(HPO_4)^{2-}$  was the most prevalent phosphatocomplex form present in solution at high temperatures. Table VII summarizes the thermochemical properties of the

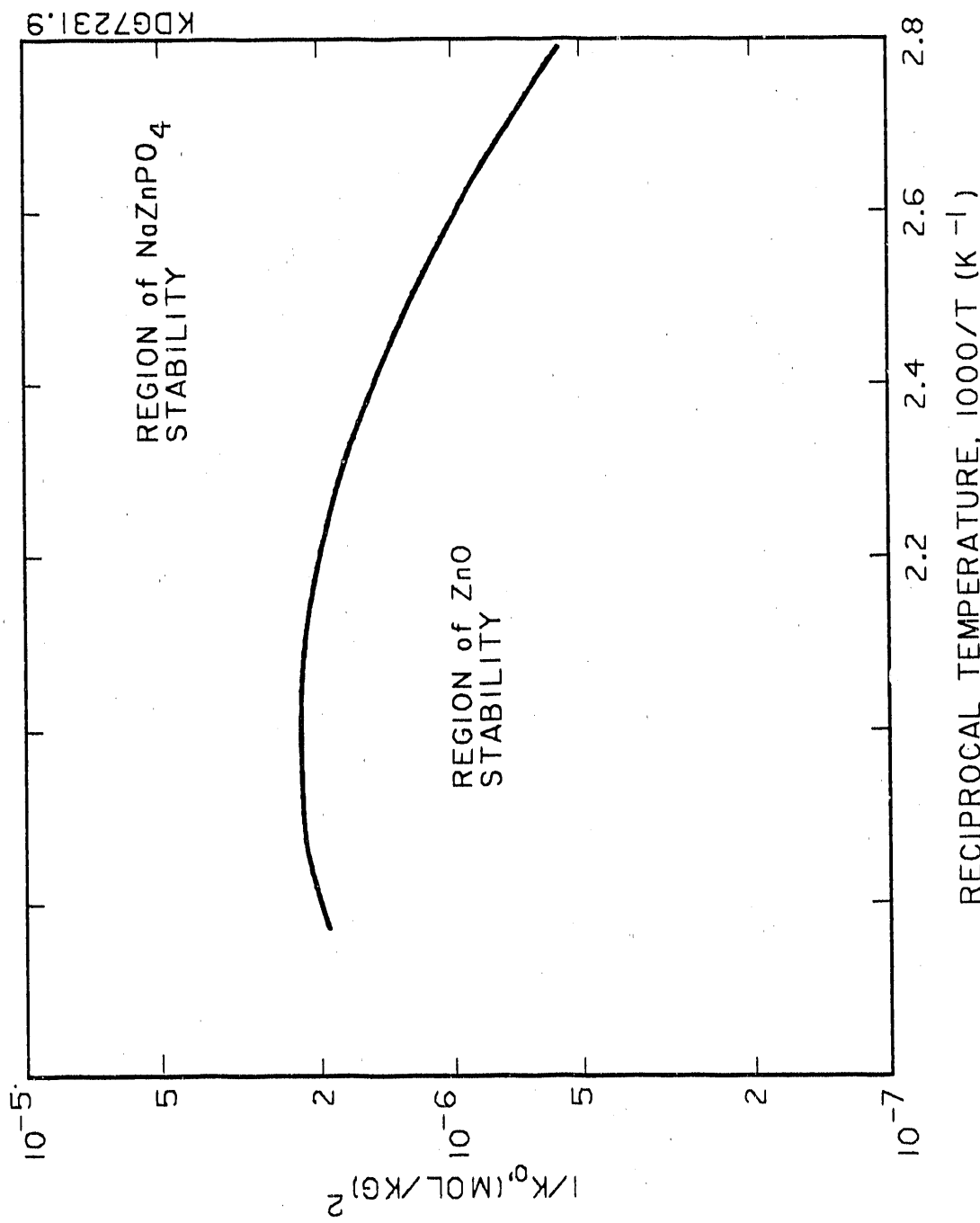


Figure 9. Predicted Phase Boundary for  $\text{ZnO}/\text{NaZnPO}_4$  Transformation in Aqueous Sodium Phosphate Solutions.

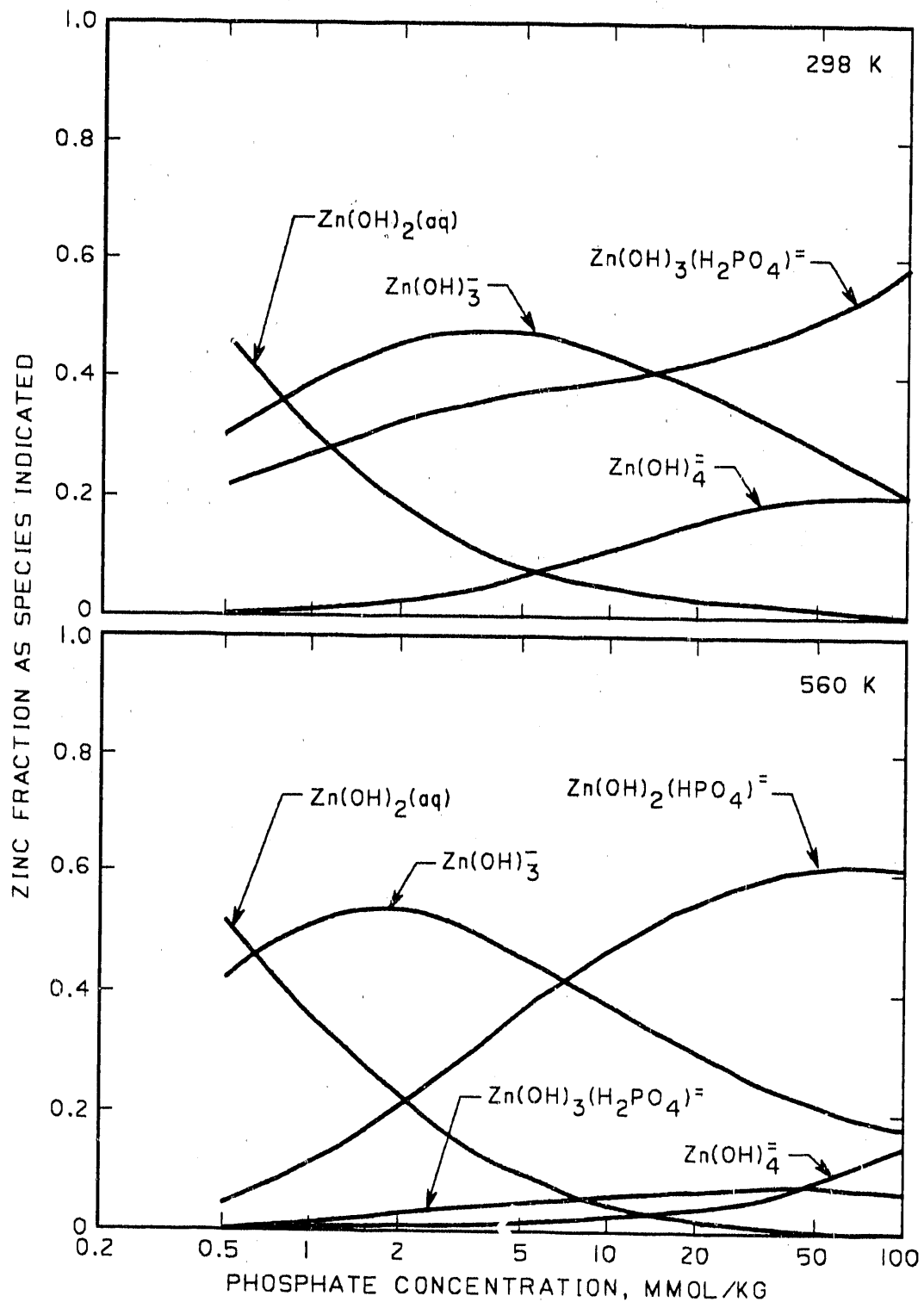


Figure 10. Distribution of Zn(II) Ion Complexes Present in Solution at 298 K (Top) and 560 K (Bottom). (N/P = 2.3).

TABLE VII. Thermochemical Parameters for Phosphate-Based Species  
in the ZnO-Na<sub>2</sub>O-P<sub>2</sub>O<sub>5</sub>-H<sub>2</sub>O System

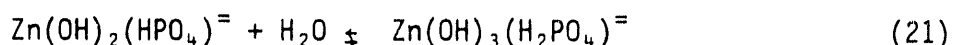
Species	$C_p^\circ(298)^*$ $\text{J}\text{-mol}^{-1}\text{-K}^{-1}$	$S^\circ(298)^*$ $\text{J}\text{-mol}^{-1}\text{-K}^{-1}$	$\Delta H_f^\circ(298)$ $\text{kJ}\text{-mol}^{-1}$	$\Delta G_f^\circ(298)$ $\text{kJ}\text{-mol}^{-1}$	Reference Cited
Na(s)	28.2	51.21	0	0	20
Na <sup>+</sup> (aq)	-28	41.0	-240.12	-261.92	20
P(s)	23.8	41.1	0	0	20
PO <sub>4</sub> <sup>3-</sup> (aq)	-283	-153.6	-1277.4	-1018.8	20, 21
HPO <sub>4</sub> <sup>2-</sup> (aq)	-112	-32.6	-1305.5	-1089.7	13, 21
H <sub>2</sub> PO <sub>4</sub> <sup>-</sup> (aq)	37	72.4	-1308.8	-1130.8	12, 21
NaZnPO <sub>4</sub> (s)	150.3	98.7	-1650.0	-1517.3	This Work
Zn(HPO <sub>4</sub> ) <sup>0</sup> (aq)	-	-	-	-1248.4	8
Zn(H <sub>2</sub> PO <sub>4</sub> ) <sup>+</sup> (aq)	-	-	-	-1285.2	9
Zn(OH) <sub>2</sub> (HPO <sub>4</sub> ) <sup>=</sup> (aq)	-115.9	145.5	-1889.1	-1613.9	This Work
Zn(OH) <sub>3</sub> (H <sub>2</sub> PO <sub>4</sub> ) <sup>=</sup> (aq)	-	57.1	-2234.8	-1863.8	This Work

\* Ionic heat capacities and entropies are referred to an absolute scale where  $C_p^\circ(\text{H}^+) = -71 \text{ J}\text{-mol}^{-1}\text{-K}^{-1}$  and  $S^\circ(\text{H}^+) = -22.2 \text{ J}\text{-mol}^{-1}\text{-K}^{-1}$  (see Table VI).

presently known species in the  $ZnO-Na_2O-P_2O_5-H_2O$  system based on the Table V equilibria and tabulated thermochemical properties of  $H_2PO_4^-$ ,  $HPO_4^{2-}$ , and  $PO_4^{3-}$ .

As calculated from Table VII,  $\Delta G^\circ(298)$  for complexing the  $HPO_4^{2-}$  ion with the  $Zn^{+2}$  and  $Zn(OH)_2(aq)$  ions is -11.4 and  $-4.50 \pm 2.25$  kJ, respectively. Thus, hydrolysis does not appreciably shift these phosphatocomplexing equilibria. The highly positive entropy change determined for the latter complexing reaction is indicative of phosphatocomplex stability at elevated temperatures (see Figure 10). Similar behavior was also observed for the  $Cu(OH)_2(HPO_4)^2-$  phosphatocomplexing reaction.<sup>(10)</sup>

The presence of an additional  $Zn(II)$  ion phosphatocomplex,  $Zn(OH)_3(H_2PO_4)^2-$ , was indicated at lower temperatures.  $\Delta G^\circ(298)$  values for forming  $H_2PO_4^-$  ion complexes with the  $Zn^{+2}$  and  $Zn(OH)_3^-$  ions, however, differ appreciably: -7.1 vs.  $-34.9 \pm 2.2$  kJ. This result indicates that hydrolysis promotes stability of  $Zn(II)-H_2PO_4^-$  complexes at low temperatures. The crossover point at which concentrations of the high temperature phosphatocomplex exceed those of the low temperature phosphatocomplex is determined by evaluating the equilibrium:



This equilibrium is independent of phosphate concentration and depends only on temperature; TABLE VII values indicate that the high temperature form dominates above 378 K.

## REFERENCES

1. C. F. Baes and R. E. Mesmer, The Hydrolysis of Cations, John Wiley & Sons, New York 1976.
2. I. L. Khodakovskii and A. E. Elkin, Geokhimiya 10, 1490 (1975).
3. A. O. Gubeli and J. Ste-Marie, Can. J. Chem. 45, 827 (1967).
4. E. Thilo and I. Schulz, Z. anorg. allg. Chemie, 265, 201 (1951).
5. A-W. Kolsi, A. Erb and W. Freundlich, C. R. Acad. Sci. 282, Ser. C-575 (1976).
6. S. E. Ziemniak, M. E. Jones and K. E. S. Combs, J. Solution Chem. 18, 1133 (1989).
7. H. Ohtaki, T. Yamaguchi and M. Maeda, Bull. Chem. Soc. Japan 49, 701 (1976)
8. H. Sigel, K. Becker and D. B. McCormick, Biochim. Biophys. Acta 148, 655 (1967).
9. C. W. Childs, Inorg. Chem. 9, 2465 (1970).
10. S. E. Ziemniak, M. E. Jones and K. E. S. Combs, Knolls Atomic Power Laboratory Report, KAPL 4715 (1990).
11. F. H. Sweeton, R. E. Mesmer and C. F. Baes, J. Solution Chem. 3, 191 (1974).
12. R. E. Mesmer and C. F. Baes, J. Solution Chem. 3, 307 (1974).
13. N. C. Treloar, Central Electricity Research Laboratory Report RD/L/N 270/73 (1973). (see WAPD-TM-1302, March 1979).
14. W. L. Marshall and E. V. Jones, J. Phys. Chem. 70, 4028 (1966).
15. D. L. Marquardt, J. Soc. Indust. Appl. Math. 2, 431 (1963).
16. P. Schindler, H. Althaus, F. Hofer and W. Minder, Helv. Chim. Acta 48, 1204 (1965).
17. O. Kubaschewski and C. B. Alcock, Metallurgical Thermochemistry, Pergamon Press, Oxford (1983).
18. C. M. Criss and J. W. Cobble, J. Amer. Chem. Soc. 86, 5390 (1964).
19. M. H. Abraham and Y. Marcus, J. Chem. Soc., Faraday Trans. 1, 82, 3255 (1986).
20. D. D. Wagman et al., J. Phys. Chem. Ref. Data, 11, Suppl. 2 (1982).
21. J. W. Larson, K. G. Zeeb and L. G. Hepler, Can. J. Chem. 60, 2141 (1982).

**END**

**DATE FILMED**

**01/30/91**

